Energy-Time Entanglement Preservation in Plasmon-Assisted Light Transmission

Sylvain Fasel,[1,*] Franck Robin,[2] Esteban Moreno,[3] Daniel Erni,[2] Nicolas Gisin,[1] and Hugo Zbinden[1]

[1]*Group of Applied Physics, University of Geneva, CH-1211 Geneva 4, Switzerland*

[2]*Communication Photonics Group, ETHZ, 8092 Zürich, Switzerland*

[3]*Departamento de Fisica Teorica de la Materia Condensada, Universidad Autonoma de Madrid, E-28049 Madrid, Spain*

(Received 11 October 2004; published 21 March 2005; corrected 7 April 2005)

We report on experimental evidence of the preservation of the energy-time entanglement of a pair of photons after a photon-plasmon-photon conversion. This preservation is observed in two different plasmon conversion experiments, namely, extraordinary optical transmission through subwavelength metallic hole arrays and long range surface plasmon propagation in metallic waveguides. Plasmons are shown to coherently exist at two different times separated by much more than their lifetimes. This kind of entanglement involving light and matter is expected to be useful for future processing and storing of quantum information.

DOI: 10.1103/PhysRevLett.94.110501 PACS numbers: 03.67.Mn, 42.50.Dv, 71.36.+c, 73.20.Mf

Entanglement is one of the most fundamental aspects of the quantum theory. While it is somewhat counterintuitive and has no classical counterparts, it can be used to achieve information and communication tasks with much higher efficiencies than otherwise possible classically, and is thus the heart of the quantum information. A particular form of entanglement, the energy-time entanglement involving photons at telecom wavelength, is particularly efficient in carrying quantum information over large distances as it has been shown to be specially robust against environmental perturbation [1]. This already leads to applications such as quantum cryptography [2] or quantum teleportation [3]. However, entanglement involving distant solid matter is a mandatory but difficult step for useful quantum information processing and storing, and researches are held in that direction [4–7]. Interaction between energy-time entangled photons at telecom wavelength and quantum states of matter is thus of great interest, both from a fundamental point of view and for its potential future applications.

We investigate the coupling of energy-time entangled photon pairs with surface plasmon (SP) polaritons, which are a collective excitation wave involving typically 10^{10} free electrons propagating at the surface of conducting matter (usually metal) [8]. To this end, perforated gold film and gold stripe embedded in dielectric were successively placed in the path of energy-time entangled photons. Indeed, these types of metallic structure each allow light to be converted into SPs.

In this Letter, we present evidence that energy-time entanglement survives this photon-plasmon-photon conversion with photons at telecom wavelength. To this end, we measure the strength of nonlocal quantum correlations involving photons from entangled pairs, using a Franson-type interferometric experiment [9]. We measured it in the case that both photons go directly to the interferometers, and in the case that one member of the entangled pair undergoes a plasmon conversion before reaching its interferometer. The strength of the quantum correlation is quantified by means of the visibility of interferences fringes, recorded in both cases. We show that no visibility reduction is observed and thus that entanglement is preserved.

Let us first consider the setup including the gold films perforated with periodic subwavelength hole array. This kind of nanostructure impedes the direct photon transmission, but allows the resonant excitation of a SP either at the front, back, or at both opposite metal interfaces (depending on the adjacent dielectrics), which reradiates a photon at the back side of the metallic film. The transmittance (normalized to the holes' area) of the hole array is typically 1 order of magnitude larger than the normalized transmittance for single subwavelength apertures [10]. This phenomenon, called extraordinary optical transmission [11–14], is known to preserve polarization entanglement under certain geometric conditions [15,16].

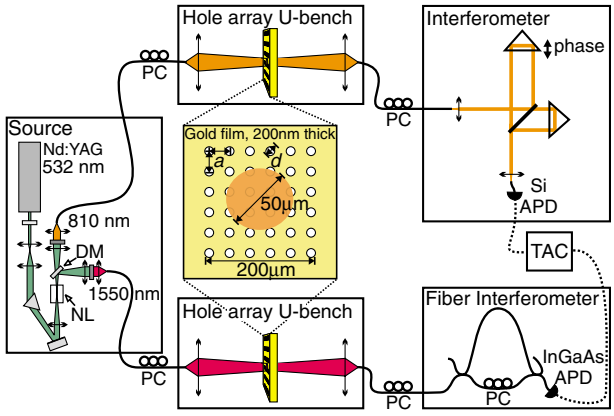

FIG. 1 (color online). Schematic of the experimental setup. One hole array is inserted at a time either in the 810 nm or in the 1550 nm designated U-bench. NL, nonlinear crystal; DM, dichroic mirror; PC, polarization controller; TAC, time to analog converter; APD, avalanche photodiode; *a*, lattice periodicity; *d*, hole diameters (see text).

The experimental setup is made of a photon pairs source, two U-benches allowing the two different perforated gold film samples to be inserted and removed alternatively in the paths of the photons, and two interferometers (see Fig. 1). The photon pairs are created inside a $KNbO_3$ nonlinear crystal pumped with a 532 nm Nd-doped yttrium aluminum garnet (Nd:YAG) continuous laser (coherence length >1 km) in a type I spontaneous parametric down conversion (SPDC) configuration. One member of the pair has its central wavelength around 810 nm with a spectral width of about 2 nm, while the other is centered around 1550 nm with a spectral width of 7 nm. These values correspond to coherence times of 1.1 ps and coherence lengths of 0.34 mm. Adjusting the phase matching by tilting the crystal, it is possible to tune slightly these central wavelength. The SPDC generated photons are collected into two single mode fibers by means of a dichroic mirror and two coupling lenses and sent to the U-benches. The properties of hole arrays designed to match either the 810 nm or the 1550 nm photons are investigated successively, using the corresponding specially designed U-benches. The photons that undergo the plasmonic conversion are thus either the 810 nm one or the 1550 nm ones, only one hole array being investigated at a time.

The U-benches are each made of two lenses. The first focuses the light at the output of the first single mode fiber into a beam with a 50 μm beam diameter situated a few centimeters away from the lens. The second lens couples back this beam inside another single mode fiber that is finally connected to an interferometer. Perforated gold film samples can be held at the beam waist position perpendicularly to the beam optical axis, by an orientable mount. Without samples, the U-benches feature about 3 dB insertion losses, without measurable spectral or polarization dependency. When a sample is inserted into the photon beam, no corrections are made to the lenses alignment. The light that is collected back into the fiber is therefore the light which is reemitted in the same spatial mode than in the case where no sample is inside the beam. Control of the incident polarization state is made using the fiber polarization controller in front of the U-benches. However, as expected in this particular square hole array configuration for which one can assume that photons arrive perpendicularly to the sample (less than 1 degree of angular spreading), the polarization dependency of the transmittance at the operating wavelength was observed to be less than 2 dB. The other polarization controllers are used to control the polarization at the input of both interferometers and inside the fiber interferometer in order to maximize the optical visibility.

The output of the U-benches are each connected to unbalanced Mach-Zender interferometers, both with 1 m optical path length difference between the two arms (this correspond to a time difference of 3.3 ns). The photons independently travel through the long arm and short arms of their respective interferometers and have a 50% probability of both choosing the long arms or both the short arms of their respective interferometers. These events are undistinguishable, provided (1) the path length differences of the interferometers are identical within the coherence length of the photons; (2) the coherence length of the pump laser is much larger than this imbalance. This leads to quantum interferences that correlate the chosen output port for both photons. By measuring the time differences between the detections of both photons from a pair with a time to analog converter, and using a time window discriminator, it is possible to isolate the interfering events from the noninterfering ones (i.e., photons choose different arms), as they happen at different times. Counting the interfering events as a function of the sum of the phases applied inside the interferometers leads to interference fringes of which visibility is a direct indication of the strength of the quantum correlation due to the energy-time entanglement. This can be used to verify that the energy-time entanglement is not destroyed by the photon-plasmon-photon conversion [9].

The interferometer designed for the 810 nm photons is made out of bulk optics, while the other is made out of fibers. Both interferometers are passively stabilized by means of temperature regulation. The 810 nm photons are detected at one output of the bulk interferometer using an actively quenched silicon avalanche photodiode (APD) photon counter (EG&G). The 1550 nm photons are detected at one output of the fiber interferometer using an InGaAs APD photon counter (idQuantique), gated with the properly delayed detection signal of the silicon counter. In this experiment the sum of the phases is adjusted by tuning the length of the long arm of the bulk interferometer using a piezoelectric actuator. The width of the time window discriminator is about 1 ns. The dark counts of the InGaAs APD are measured to be about 3.5×10^{-5} counts per gate. The dark counts of the Si APD is negligible. More details about the source, the interferometers, and the measurement process can be found in [17,18].

The two different perforated film samples were fabricated in 200-nm-thick evaporated gold films on 0.9 mm glass substrates. The gold was coated with a 200-nm-thick PMGI (polydimethyl glutarimide) electron-beam sensitive resist layer which was patterned using electron-beam lithography. Following exposure of the hole arrays, the resist was developed in tetraethylammonium hydroxide for 1 min at 22 °C and rinsed with deionized water. The structures were then transferred into the Au layer using Ar sputtering for 14 min with 200 W power. Finally, the PMGI residuals were removed using oxygen ashing. The arrays' size is about 200×200 μm^2. The holes are circular and disposed following a regular square pattern. As the light beam area is only about 5% of the array area, the array can be considered as infinite, and the boundary effects are thus negligible.

In our samples, the extraordinary optical transmission is mediated by SP mode lying at the metal-substrate interface and propagating along the square array diagonals. In order to determine the optimal periodicity a and hole diameter d for maximal transmittance enhancement (i.e., for optimal coupling of the SPs to the photon pair's members at the corresponding wavelengths) various simulations were performed employing a modal expansion method in connection with surface impedance boundary conditions on the metal interfaces, and perfect metal boundary conditions in the hole walls [14]. Several hole arrays were fabricated, with slight changes around theoretical values and for a range of fabrication parameters. They were characterized for transmittance spectra, using classical light spectrometry.

Results exhibit the typical shapes of SPs extraordinary light transmission, featuring resonances due to SPs excitations (see Fig. 2). Verifications were made to confirm that the reemitted light originates from photon-plasmon-photon conversions. First, the resonance position scales linearly with the array period, while the peaks' height and width depend on the hole diameter. Second, the SP band structure was recovered by changing the polarization and incident angle of the impinging photons. We explain the peak's positions dependency on hole diameters (visible in Fig. 2) by the fact that the electromagnetic mode responsible for the transmission is not the bare SP of a flat metal surface, but rather the SP perturbed by the holes, i.e., the SP of a corrugated surface. The dispersion relation of this mode changes slightly with the hole size, and therefore the resonance position also shifts. Note that, as is to be expected, the larger the hole, the larger the resonant wavelength and the resonance width. Results were very similar to the one usually found in the literature on the subject [11–13,15].

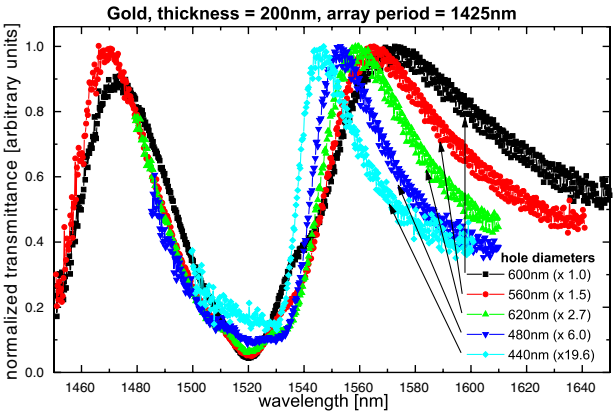

FIG. 2 (color online). Transmittance spectra of some hole arrays designed for transmission at 1550 nm (spectra of the samples designed for 810 nm have similar shapes). They shows mainly the dependencies of the peaks width with the hole diameters. Peaks' heights are normalized by factors shown in between brackets in the legend. The small fast oscillations correspond to Fabry-Perrot effects at the glass substrate interfaces.

From these measurements, the most suited arrays with respect to our experimental limitations were chosen for the entanglement experiment. The exact operating wavelengths λ were chosen accordingly. Entanglement measurements for the two wavelengths were made separately. First, the source was tuned to produce photons at 820 and 1515 nm and a hole array with $a = 700$ nm and $d = 300$ nm was used. Second, the source was tuned to produce photons at 810 and 1550 nm and a hole array with $a = 1400$ nm and $d = 600$ nm was used. Interferences fringes are recorded without samples inside the U-benches in order to have a reference. The chosen sample is then inserted inside the U-bench, and its position is adjusted using red laser light. Interference fringes are then recorded again, and the ratio of the maximal count rate in both cases is verified to be compatible with the transmittance values previously measured with classical light. The net visibilities of the interferences fringes are calculated by substracting the noise level and fitting the data to a sinusoidal dependency (see Fig. 4). The noise level is measured by shifting the delay of the detection gate applied on the InGaAs photon counter to avoid detection of photon pairs. Hence, this noise is the sum of InGaAs APD dark count rate and double pair emission rate of the SPDC source that lead to uncorrelated detections.

As mentioned, in order to supplement our experiment, we performed measurements on a second kind of plasmonic device, using the same Franson-type experimental setup. The gold hole array at 1550 nm is replaced by a long range surface plasmon (LR-SP) waveguide, provided by Micro Managed Photons A/S. This waveguide consists of a 0.5 cm long gold stripe, sandwiched between two layers of benzocyclobutene, a dielectric of refraction index $n = 1.535$, and deposited upon a silicon wafer. Notice that the plasmon waveguide (length 5 mm) is much longer than the single photon coherence length (0.34 mm in air), or, in other terms, the propagation time of the plasmon across the waveguide is much longer than the coherence time of the photon. Hence during a certain time the photons are completely converted into plasmons. The gold stripe is 8 μm wide and about 20 nm thick. Standard single mode fibers are approached as close as possible from the ends of the

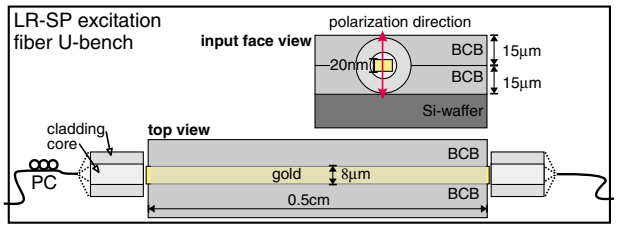

FIG. 3 (color online). Schematic of the fiber U-bench used to excite LR-SP propagation through gold stripe waveguide. BCB, benzocyclobutene.

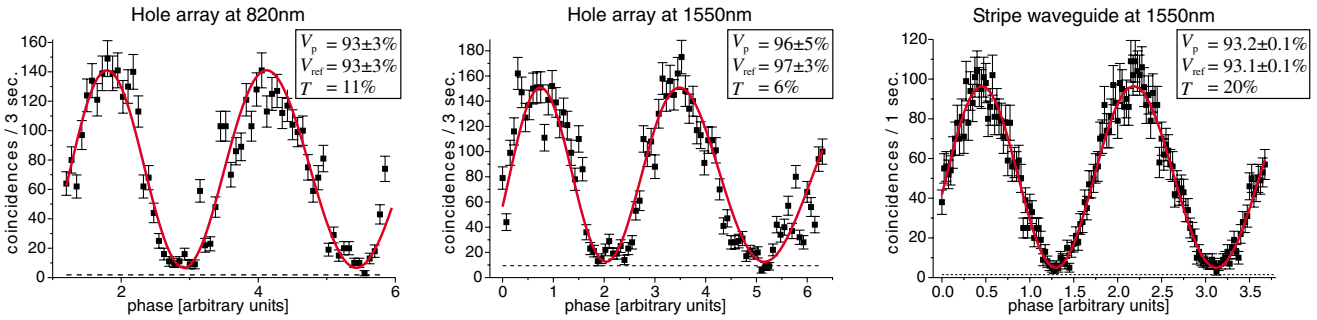

FIG. 4 (color online). Interference fringes recorded for the three experiments. V_p, net visibility of the shown fringes (with plasmonic conversion); V_{ref}, reference net visibility (without plasmonic conversion); T, transmittance of the plasmonic device. The dashed horizontal line is the noise level (see text for details).

gold stripe. The polarization mode is set to be linear and perpendicular to the surface sample by mean of a fiber polarization controller. LR-SPs propagate along the gold stripe and reemit light which is collected by another single mode fiber (see Fig. 3). More details about this gold stripe device and this particular plasmonic excitation procedure can be found in Ref. [19], and references therein.

From our results (summarized in Fig. 4), one can see that the strength of the quantum correlations and thus the entanglement are clearly preserved by the photon-plasmon-photon conversion, at the two working wavelengths. No relevant two-photons interference visibility reductions occur when a sample is inserted in the path of a photon beam. The only effect is the reduction of the coincidence count rate due to the partial transmittance resulting from extraordinary light transmission. Energy-time entanglement is thus proven to survive plasmon conversions at telecom wavelengths.

The preservation of this kind of entanglement implies that SPs are coherently created by photons being in a superposition of two different incoming times, separated by several nanoseconds, while the SPs lifetime in our experiment should be in the order of picoseconds (the time to travel through the sample thickness or waveguide length). Therefore the only SP quantum state compatible with the above results is a superposition of a single SP existing at two different moments in time, separated one from the other by a duration thousands of times longer than the its own lifetime. At a macroscopic level this would lead to a ''Schrödinger cat'' living at two epochs that differ by much more than a cat's lifetime. The plasmons of the present experiment involve a mesoscopic number of electrons of about 10^{10}. It should, however, be stressed that these do carry collectively only a single degree of freedom, i.e., a single qubit.

Apart from these fundamental considerations, our results show that energy-time entanglement can be efficiently coupled to SPs. As this kind of entanglement is robust for long distance quantum information transmission, future quantum SP circuits could be integrated with long range optical quantum communication networks.

Micro Managed Photons (MMP) A/S (Denmark) is gratefully acknowledged for providing the gold stripe LR-SP samples and expert advice. Financial support by the Swiss NCCR Quantum Photonics is acknowledged.

*Electronic address: sylvain.fasel@physics.unige.ch

[1] R. T. Thew, S. Tanzilli, W. Tittel, H. Zbinden, and N. Gisin, Phys. Rev. A **66**, 062304 (2002).
[2] N. Gisin, G. Ribordy, W. Tittel, and H. Zbinden, Rev. Mod. Phys. **74**, 145 (2002).
[3] C. H. Bennett, G. Brassard, C. Crépeau, R. Jozsa, A. Peres, and W. K. Wootters, Phys. Rev. Lett. **70**, 1895 (1993).
[4] C. Monroe, Nature (London) **416**, 238 (2002).
[5] K. Hammerer, K. Molmer, E. S. Polzik, and J. I. Cirac, Phys. Rev. A **70**, 044304 (2004).
[6] M. D. Barrett *et al.*, Nature (London) **429**, 737 (2004).
[7] J. Sherson, B. Julsgaard, and E. S. Polzik, quant-ph/0408146.
[8] W. L. Barnes, A. Dereux, and T. W. Ebbesen, Nature (London) **424**, 824 (2003).
[9] J. D. Franson, Phys. Rev. Lett. **62**, 2205 (1989).
[10] H. A. Bethe, Phys. Rev. **66**, 163 (1944).
[11] T. W. Ebbesen *et al.*, Nature (London) **391**, 667 (1998).
[12] H. F. Ghaemi, T. Thio, D. E. Grupp, T. W. Ebbesen, and H. J. Lezec, Phys. Rev. B **58**, 6779 (1998).
[13] D. E. Grupp, H. J. Lezec, T. W. Ebbesen, K. M. Pellerin, and T. Thio, Appl. Phys. Lett. **77**, 1569 (2000).
[14] L. Martín-Moreno *et al.*, Phys. Rev. Lett. **86**, 1114 (2001).
[15] E. Altewischer *et al.*, Nature (London) **418**, 304 (2002).
[16] E. Moreno, F. J. García-Vidal, D. Erni, J. I. Cirac, and L. Martín-Moreno, Phys. Rev. Lett. **92**, 236801 (2004).
[17] G. Ribordy, J. Brendel, J.-D. Gautier, N. Gisin, and H. Zbinden, Phys. Rev. A **63**, 012309 (2001).
[18] S. Fasel, G. Ribordy, H. Zbinden, and N. Gisin, Eur. Phys. J. D **30**, 143 (2004)
[19] T. Nikolajsen, K. Leosson, I. Salakhutdinov, and S. I. Bozhevolnyi, Appl. Phys. Lett. **82**, 668 (2003).